

Technical Paper
ICENES2007
June 3-8, 2007, Istanbul, Turkey

**“Benchmarking the CAD-based ATTILA Discrete Ordinates Code
with Experimental Data of Fusion Experiments and to the Results of
MCNP code in Simulating ITER ”**

Mahmoud Z. Youssef
University of California, Los Angeles, Los Angeles, CA, USA

Russell Feder
Princeton Plasma Physic Laboratory, Princeton, NJ, USA

Todd Wareing
Transpire, Inc., Gig Harbor, WA, USA

Abstract

ATTILA is a newly developed finite element, Discrete Ordinates code based on Sn neutron, gamma, and charged particle transport in 3-D geometry in which unstructured tetrahedral meshes are generated to describe complex geometry that is based on CAD input (Solid Works, Pro/Engineer, etc). In the present work we benchmark its calculation accuracy by comparing its prediction to the measured data inside three fusion-oriented experimental mock-ups bombarded with 14 MeV neutrons. The mock-ups simulate parts of the in-vessel components of the International Thermonuclear Experimental Reactor (ITER). The results are also compared to those based on MCNP calculations. In addition, the nuclear performance of the ITER MCNP “Benchmark” CAD model has been performed with ATTILA to compare its results to those obtained with CAD-based MCNP approach developed by several ITER participants. The objective of this paper is to compare results based on two distinctive 3-D calculation tools using the same nuclear data, FENDL2.1, and the same response functions of several reaction rates measured in ITER mock-ups and to strengthen the confidence of the international fusion neutronics community in the ATTILA and how it can precisely quantify the nuclear field in large and complex systems, such as ITER. ATTILA has the advantage of providing a full flux mapping visualization everywhere in one run where components subjected to excessive radiation level and strong streaming paths can be identified. The turnaround time for an ATTILA run is relatively shorter than MCNP and as such ATTILA lends itself to be a powerful calculation tool for fusion components design in which frequent changes are made.

I. Introduction and Background

Two distinctive calculation methods are used to quantify the nuclear field (neutron and gamma, n/g), fluxes in nuclear fusion systems, namely the Discrete Ordinates (DO) method and the Monte Carlo (MC) technique. In the former method, the n/g energy ranges and the angular direction are discretized (multi-group pins, S_n) and the cross-sections are approximated with series of Legendre polynomials (P_n) averaged over energy bins. Structured meshes based on orthogonal coordinates (Cartesian, cylindrical, spherical, etc.) are used to approximate complex 3D geometries. The multi-dimension DO codes, such as DANTSYS¹ and DOORS² are conventionally used to solve the Boltzmann neutron balance equation where the n/g fluxes and associated reaction rates (tritium production, damage, etc.) are calculated everywhere in the system. The latter MC method is based on stochastic processes. Millions of source particles are followed in random processes to estimate the required fluxes and associated responses at pre-selected locations (tallies). In codes, such as MCNP³, 3D complex geometries are described by combination of surfaces intersections to form bodies (zones). Point-poise nuclear data are used.

Deterministic codes have the advantages of: (1) fluxes and responses are calculated everywhere. Flux moments from one run can be used to calculate any additional responses, as needed and (2) shorter time to run a case compared to the Monte Carlo methods. However, the disadvantages inherited in these codes are: (1) large disk space is required to store angular fluxes, (2) ray effect due to angular discretization, and (3) cross sections should be self- shielded

particularly in resonance regions. On the other hand, the Monte Carlo codes have the advantages of having the ability to accurately model complex geometries. However, extensive effort is needed to generate the appropriate “geometry cards”. There is currently an extensive effort to use CAD-based software to represent the details of these complex geometries and then directly (by calling upon MCNP modules) or indirectly (by generating the geometry cards) assess the nuclear field in the system⁴⁻⁶. In addition, point-wise nuclear data are used as opposed to multi-group data in DO codes with the inherited approximation of averaging the data within each group. The disadvantages of these codes however are: (1) fluxes and responses are calculated at pre-selected locations hence the required responses can be calculated only at limited number of locations/regions, (2) visualization of the responses in the whole system is hard to realize, and (3) the statistical uncertainties associated with the method require careful use of variance reduction techniques.

To ensure meeting Quality Assurance (QA) requirements, the International Thermonuclear Experimental Reactor (ITER) Management and Quality Program (MQP) adopted a certain number of codes and data to perform the needed nuclear analyses. The Monte Carlo transport code, MCNP³, is the reference calculation tool (versions 4b, 4c, 5). The nuclear data bases, which are basically constructed from the Fusion Evaluated Nuclear Data Library⁷, FENDL2.1, either in multi-group (MG/GENDF, MG/MATXS) is the reference data base. It has been proposed that the Discrete Ordinates code, ATTILA, be used as a potentially quicker alternative to the MCNP code for the neutronics studies of various fusion components of ITER.

ATTILA⁸ is a newly developed finite element DO code based on S_n neutron, gamma, and charged particle transport in 3D geometry. Complex configurations of any shape are first described by the currently available CAD software packages such as Solid Works and Pro/Engineer and then used as input to ATTILA. Unstructured tetrahedral meshes are generated whose number depends on the level of details needed to accurately describe the configuration. This code was recently introduced to the fusion community.⁹ It was used to calculate the nuclear field in selected fusion-oriented design geometries and calculations were compared to MCNP results.¹⁰ As described by the code developers, ATTILA has several features as last collided flux option for post processing, integrated depletion Module for activation calculation, automated weight windows generation, user control over grid resolution, and post graphic and visualization in the entire system.

ATTILA has gone through validation procedures in order to be accepted as one of the design tools for ITER. Recently¹¹⁻¹², ATTILA has been benchmarked against the experimental data and the MCNP results in several fusion-oriented integral experiments¹³⁻¹⁴ performed at the Fusion Neutron Generator (FNG) facility¹⁵, Frascati, Italy. Furthermore, it has been benchmarked against the theoretical predictions of MCNP in large and complex systems, such as ITER. In this regard, the ITER neutronics community has selected a CAD model of the entire ITER machine represented by a 40-degree 3-D sector in which all the details of ITER components have been preserved (blanket shield modules, BSM, divertor cassettes, TF, PF, and OH coils, vacuum vessel, upper, equatorial and lower ports, etc.) Results of the CAD-based MCNP calculations (as obtained by the University of Wisconsin UW-US, FZK Germany, JAEA Japan, and ASIPP China) are inter-compared⁶ among each other and to ATTILA’s results (present work.)

In this paper we present the benchmarking results of ATTILA with the experimental data of a bulk shielding experiment and review the pertaining results¹¹⁻¹² of its benchmarking to two other

fusion-oriented experiments¹³⁻¹⁴. We also report some of the results of benchmarking ATTILA with the 40-degree sector of ITER CAD model. This will shed light on the accuracy of the prediction of ATTILA and its applicability as a nuclear design tool in fusion applications.

II. Benchmarking ATTILA

II.A Benchmarking with Fusion-oriented Integral Experiments

II.A.1 Experiments

The experimental mock-ups simulate parts of ITER in-vessel components, namely: (1) the tungsten mockup configuration¹⁴, (2) the steaming mock-up configuration¹³, and (3) the bulk shielding mock-up configuration. In the last two mock-ups, the ITER blanket shielding module is simulated and is followed by a super conducting magnet (SCM) region simulated by alternating layers of SS316 and copper. In the steaming mock-up, a high aspect ratio rectangular streaming channel was introduced to simulate steaming paths between ITER blanket modules which ends with a rectangular cavity. Tungsten is used in the first experiment since it is an important plasma facing component (PFC) material in ITER. The experiments were performed at the Fusion Neutron Generator (FNG) facility¹⁵, Frascati, Italy.

The configuration of the tungsten experiment is shown in Figs 1 and 2. The 14 MeV point source is placed at a 5 cm distance from the front edge and several reactions rates were measured along the central axis at the locations shown. They are $Zr^{90}(n,2n)$, $Ni^{58}(n,2n)$, $Nb^{93}(n,2n)$, $Al^{27}(n,\alpha)$, $Fe^{56}(n,p)$, $Ni^{58}(n,p)$, $In^{115}(n,n')$, and $Au^{197}(n,\gamma)$. The first two reactions have very high threshold (~ 12 MeV). The thresholds for the next five reactions are: ~ 9 MeV, ~ 5 MeV, ~ 3 MeV, ~ 0.5 MeV, and ~ 0.2 MeV, respectively. The last reaction occurs at all energies with several resonances. It is therefore expected that the accuracy in predicting these reactions is a good measure of how well the neutron spectrum and energy-dependent reactions rates are predicted.

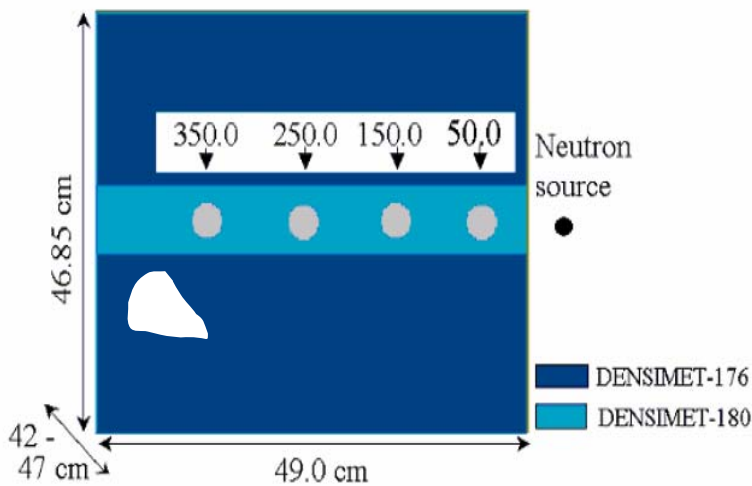


Fig. 1. The rectangular tungsten block and locations of neutron source and measured data (dimension of 4 measuring locations shown are in mm)

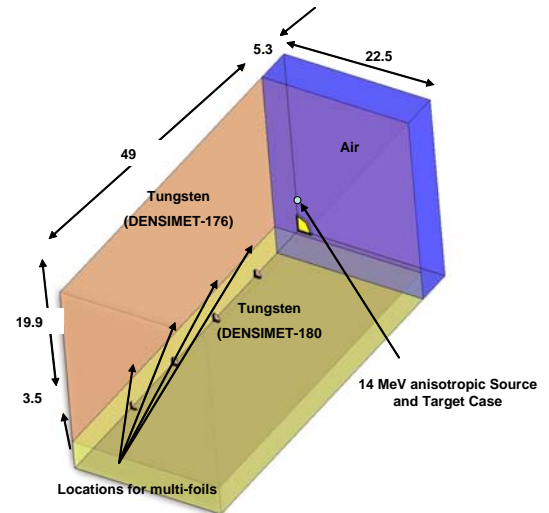


Fig. 2. The SolidWorks CAD model used in ATTILA for the tungsten experiment (1/4 of the model is shown due to symmetry)

The second experiment focuses on studying the effect of the presence of steaming paths (penetrations) in fusion devices and the ability to predict their influence on the nuclear field. The mockup (see Figs 3 and 4) resembles the ITER blanket shield module, SBM, (simulated by alternating layers of SS316 and Perspex material to simulate water) followed by the SCM region. Several reaction rates were measured along the central channel and inside the cavity at locations out-of-site of the point source and thus measure the degree of streaming through the central channel.

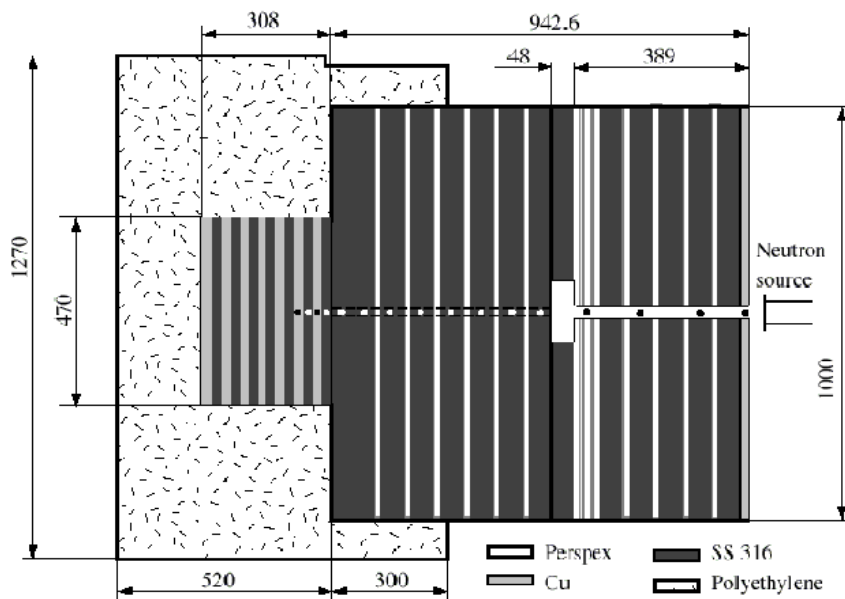


Fig. 3. The arrangement and dimensions of the steaming experiment of ITER bulk shield (dimension in mm).

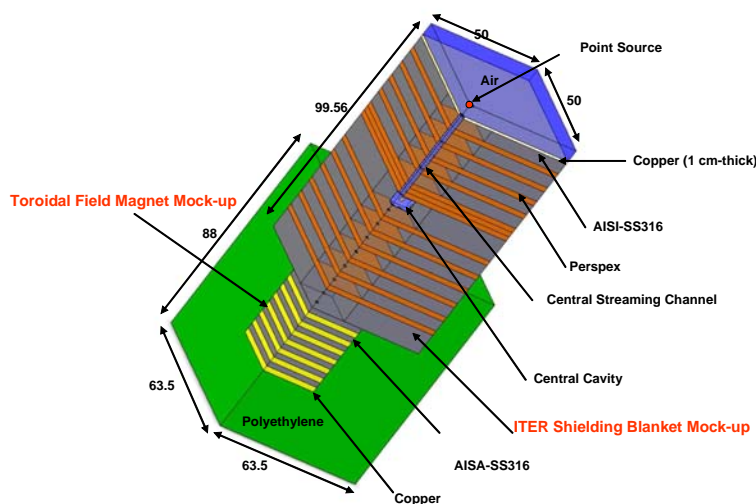


Fig. 4. . The SolidWorks CAD model used in ATTILA for the steaming experiment (1/4 of the model is shown due to symmetry)

The third experiment is the bulk shielding experiment. The configuration and material assignment are the same as in the second experiment except that the central steaming channel and the rectangular cavity are not present (see Fig. 5)

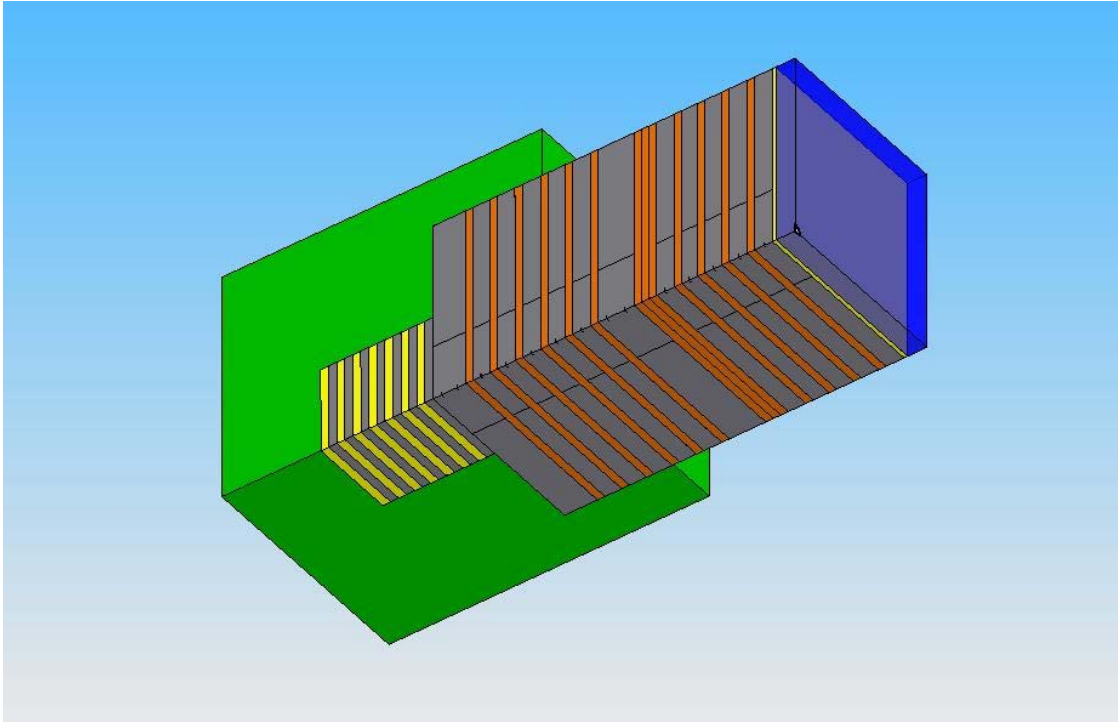


Fig. 5. The Solid Works CAD model of the bulk shield experiment. (1/4 of the model is shown due to symmetry)

Detailed description of these experiments, including anisotropic source specification, material composition, experimental and calculation results can be found in Refs. 11-12 and 16. In calculating the reaction rates, the IRDF-90 dosimetry cross-sections are used¹⁷ both in MCNP and ATTILA calculations which are based on FENDL2.1 transport data. It should be noted that the MCNP results reported here were obtained and provided by the FNG personnel.

II.A.2 Benchmarking Results

The calculated-to-experimental (C/E) values for the $\text{Ni}^{58}(n,2n)\text{Ni}^{57}$, $\text{Al}^{27}(n,\alpha)\text{Na}^{24}$, $\text{In}^{115}(n,n)\text{In}^{115m}$, and $\text{Au}^{197}(n,\gamma)\text{Au}^{198}$ along the central axis of the W-block are shown in Figs. 6-9, respectively. The C/E values for the $\text{Zr}^{90}(n,2n)\text{Zr}^{89}$, $\text{Nb}^{93}(n,2n)\text{Nb}^{92}$, and $\text{Ni}^{58}(n,p)\text{Co}^{58}$ can be found in Ref. 11. In all the reactions considered the predictions of the ATTILA are lower than MCNP results (except for $\text{Au}^{197}(n,\gamma)\text{Au}^{198}$ at the back location). The experimental and statistical errors are included in all these figures.

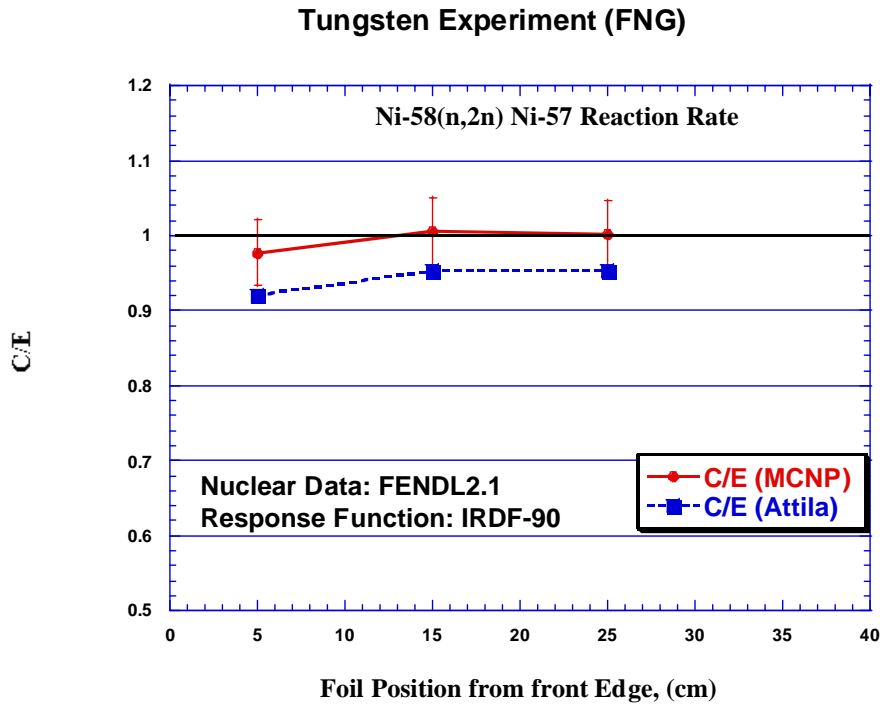


Fig. 6. The C/E values for the $\text{Ni}^{58}(n, 2n)\text{Ni}^{57}$ reaction rate along the central axis of the tungsten experiment.

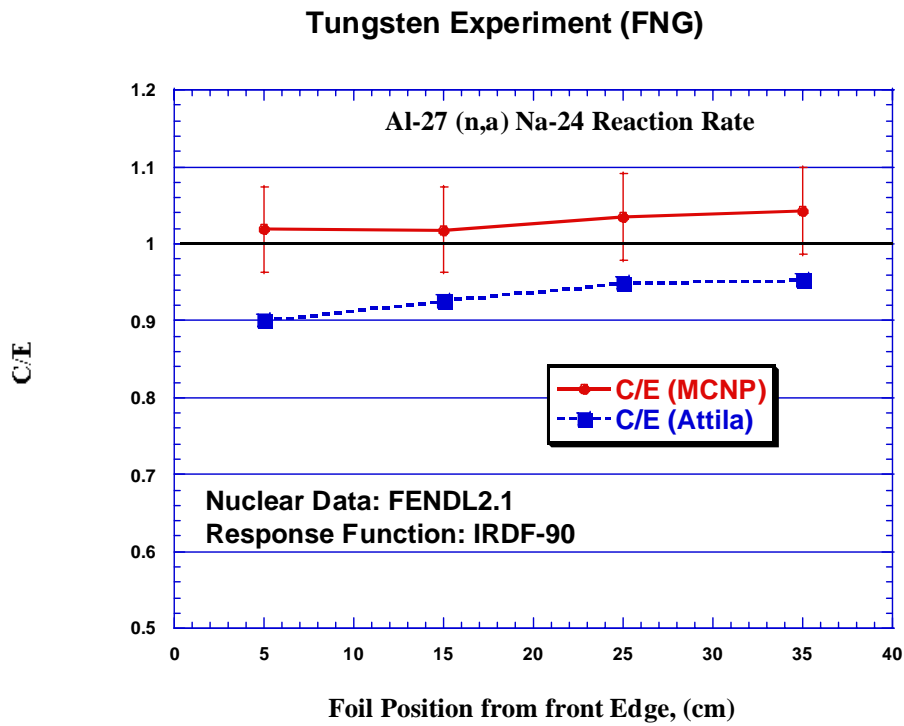


Fig. 7. The C/E values for the $\text{Al}^{27}(n,\alpha)\text{Na}^{24}$ reaction rate along the central axis of the tungsten experiment.

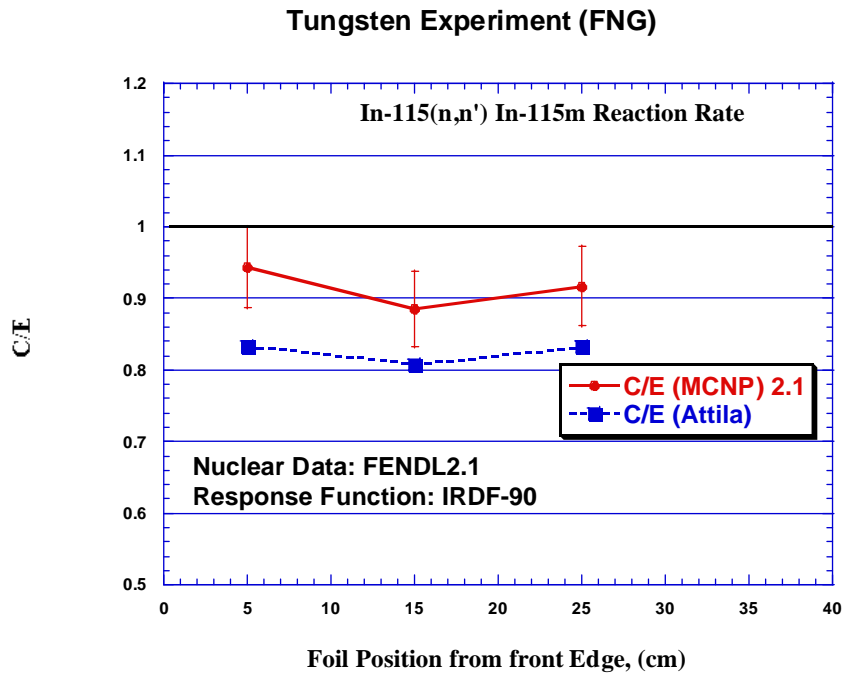


Fig. 8. The C/E values for the $\text{In}^{115}(n,n')\text{In}^{115m}$ reaction rate along the central axis of the tungsten experiment.

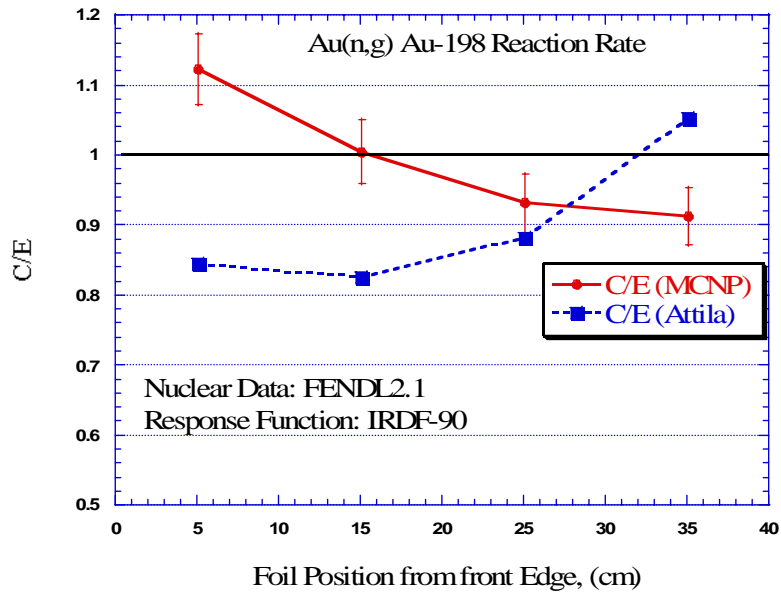


Fig. 9. The C/E values for the $\text{Au}^{197}(n,g)\text{Au}^{198}$ reaction rate along the central axis of the tungsten experiment (from Ref. 11)

The C/E values for the $\text{Nb}^{93}(\text{n},2\text{n})\text{Nb}^{92}$, $\text{Al}^{27}(\text{n},\alpha)\text{Na}^{24}$ and $\text{Au}^{197}(\text{n},\text{g})\text{Au}^{198}$ along the central axis of the streaming experiment are shown in Figs. 10,12, and 14 whereas the values inside the cavity located at the end of the central streaming channel are shown in Figs. 11,13, and 15, respectively. The upper and lower bounds of the experimental data are also indicated in these figures. The C/E values for the $\text{Ni}^{58}(\text{n},\text{p})\text{Co}^{58}$ can be found in Ref. 11. Generally, the values obtained by ATTILA are still lower than the ones obtained by MCNP both along the central channel and inside the cavity, except for the $\text{Au}^{197}(\text{n},\text{g})\text{Au}^{198}$ reaction where they are larger, as shown in Figs 14 and 15. Note that the locations where measurements were performed inside the cavity (the floor, ceiling and sides) are shown in figs. 11, 13, and 15.

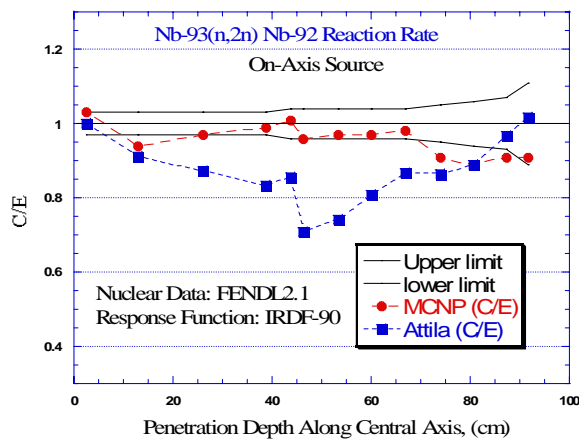


Fig. 10. The C/E values for the $\text{Nb}^{93}(\text{n},2\text{n})\text{Nb}^{92}$ reaction rate along the central axis of the streaming experiment (from Ref. 11.)

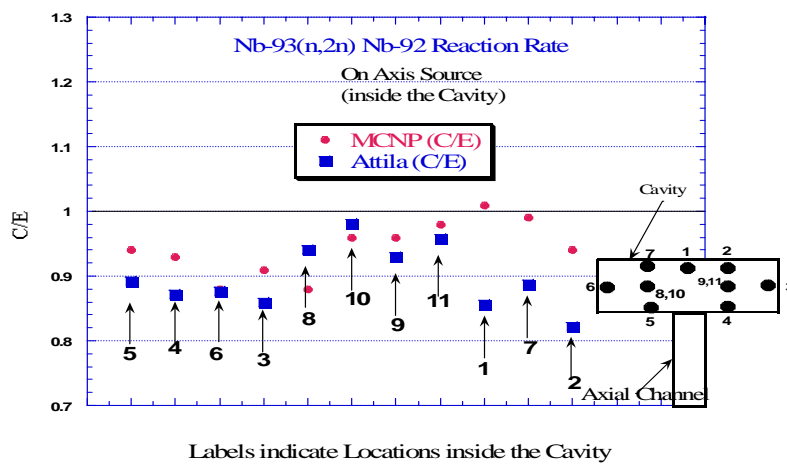


Fig. 11. The C/E values for the $\text{Nb}^{93}(\text{n},2\text{n})\text{Nb}^{92}$ reaction rate in the cavity of the streaming experiment (from Ref. 11.)

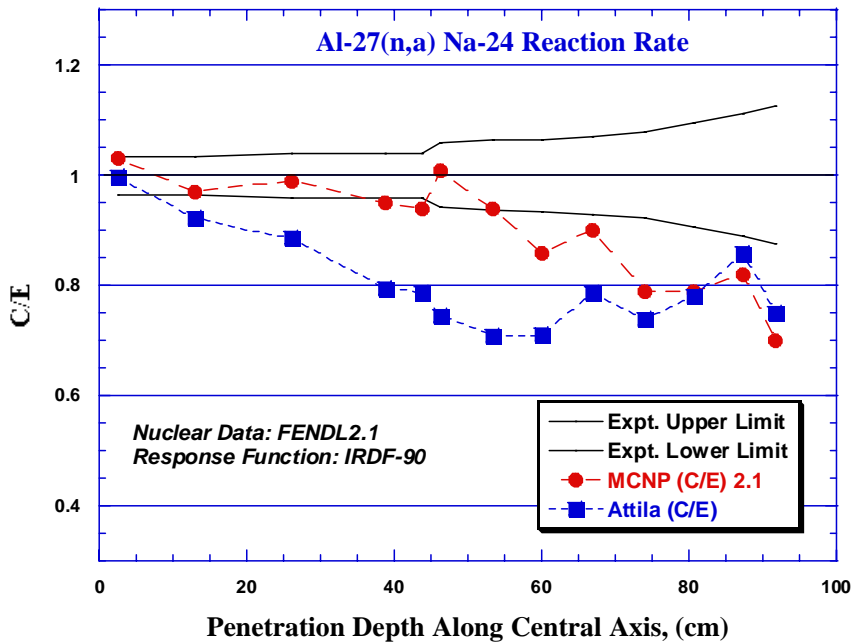


Fig. 12. The C/E values for the $\text{Al}^{27}(\text{n},\alpha)\text{Na}^{24}$ reaction rate along the central axis of the streaming experiment.

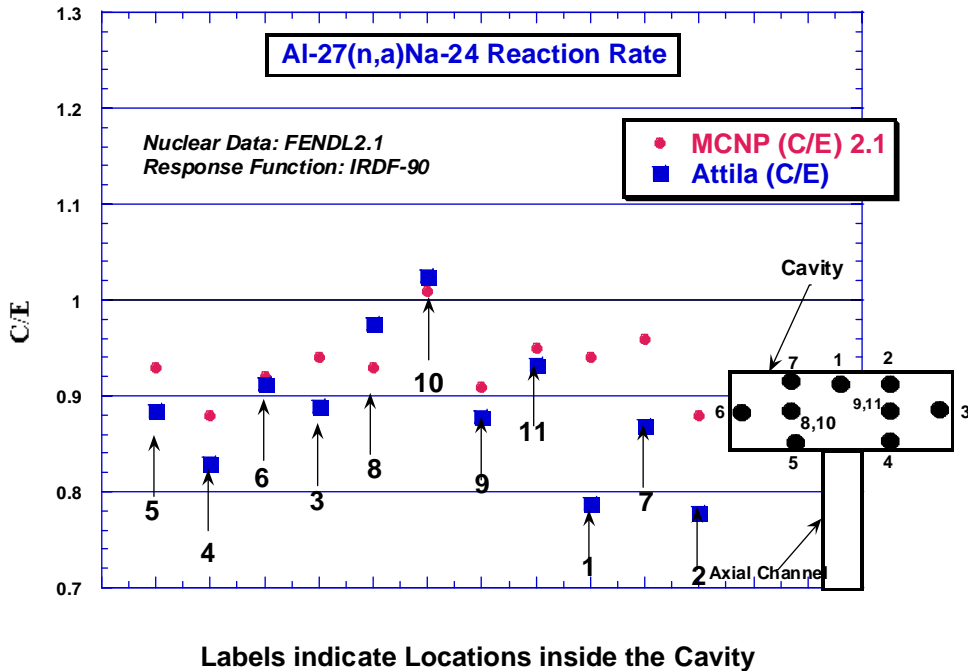


Fig. 13. The C/E values for the $\text{Al}^{27}(\text{n},\alpha)\text{Na}^{24}$ reaction rate in the cavity of the streaming experiment.

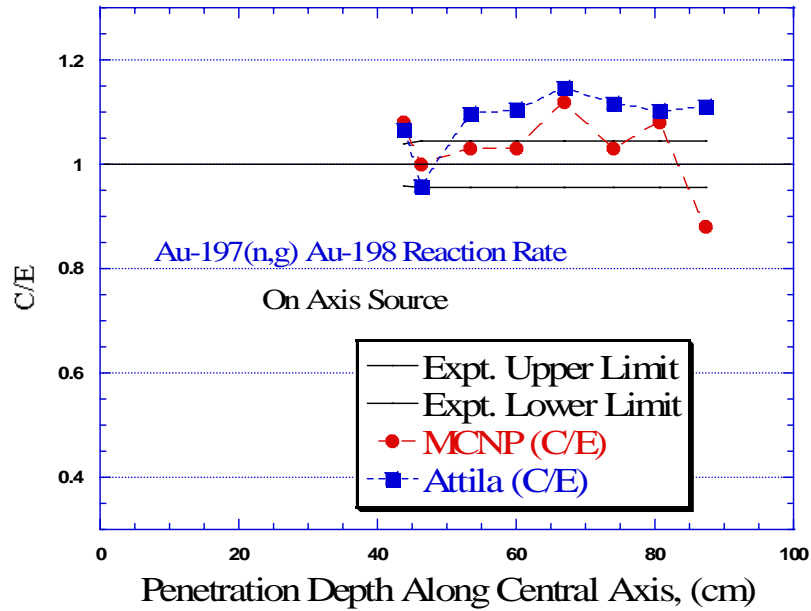


Fig. 14. The C/E values for the $Au^{197}(n, g) Au^{198}$ reaction rate along the central axis of the streaming experiment (from Ref. 11.)

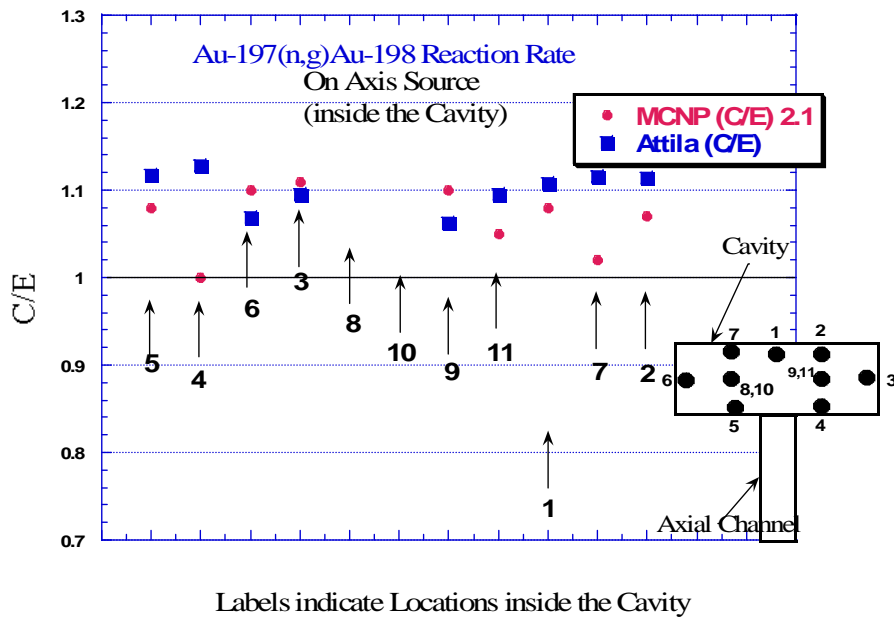


Fig. 15. The C/E values for the $Au^{197}(n, g) Au^{198}$ reaction rate in the cavity of the streaming experiment (from Ref. 11.)

The C/E values for the $\text{Nb}^{93}(\text{n},2\text{n})\text{Nb}^{92}$, $\text{Al}^{27}(\text{n},\alpha)\text{Na}^{24}$, $\text{Fe}^{56}(\text{n},\text{p})\text{Mn}^{56}$, $\text{Ni}^{58}(\text{n},\text{p})\text{Co}^{58}$, and $\text{In}^{115}(\text{n},\text{n}')\text{In}^{115\text{m}}$ along the central axis of the bulk shielding experiment are shown in Figs. 16-20, respectively. Also shown is the ratio $\text{C}(\text{ATTILA})/\text{C}(\text{MCNP})$ to indicate the deviation of ATTILA's calculations from MCNP results. This ratio is nearly unity for the $\text{Nb}^{93}(\text{n},2\text{n})\text{Nb}^{92}$ reaction (except at depth ~ 65 cm) and slightly below unity for the $\text{Fe}^{56}(\text{n},\text{p})\text{Mn}^{56}$ reaction. It is also slightly below unity for the $\text{In}^{115}(\text{n},\text{n}')\text{In}^{115\text{m}}$, $\text{Ni}^{58}(\text{n},\text{p})\text{Co}^{58}$ and $\text{Al}^{27}(\text{n},\alpha)\text{Na}^{24}$ reactions except at deep locations (see Figs. 17, 19, and 20)

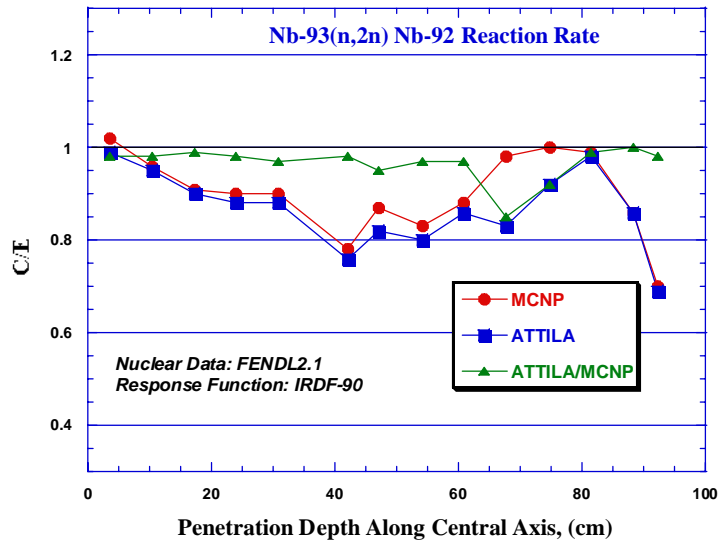


Fig. 16. The C/E values for the $\text{Nb}^{93}(\text{n},2\text{n})\text{Nb}^{92}$ reaction rate along the central axis of the bulk shielding experiment.

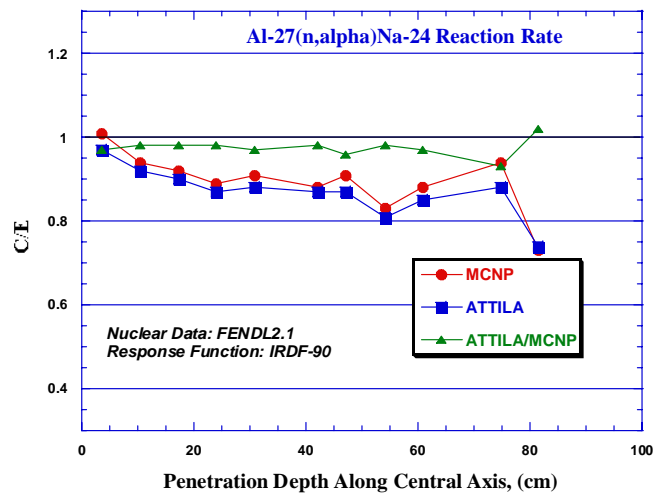


Fig. 17. The C/E values for the $\text{Al}^{27}(\text{n},\alpha)\text{Na}^{24}$ reaction rate along the central axis of the bulk shielding experiment.

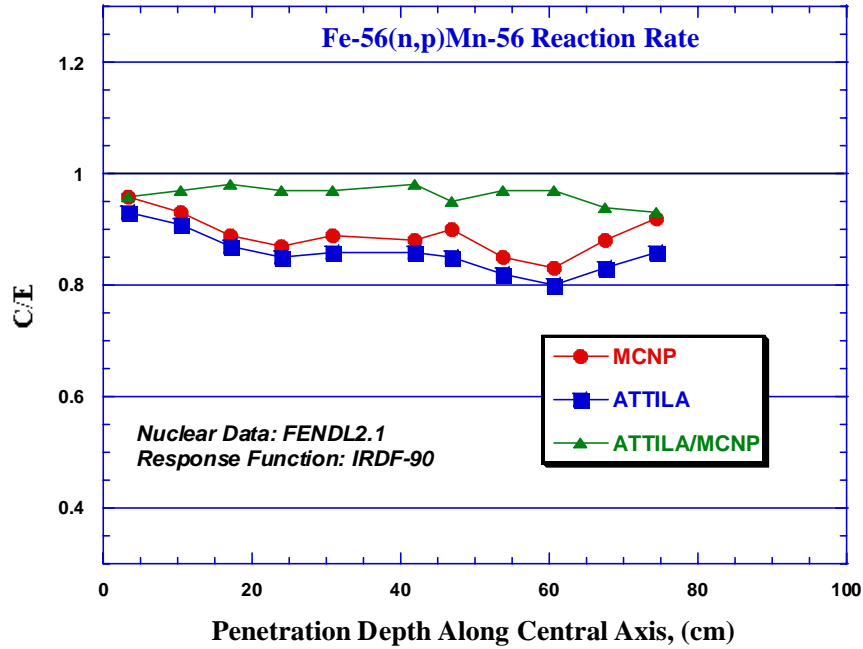


Fig. 18. The C/E values for the $\text{Fe}^{56}(\text{n,p})\text{Mn}^{56}$ reaction rate along the central axis of the bulk shielding experiment.

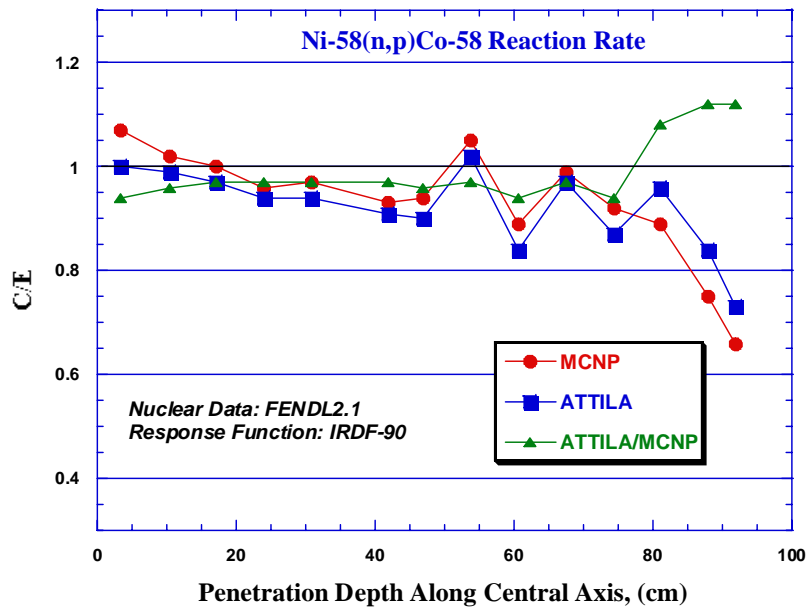


Fig. 19. The C/E values for the $\text{Ni}^{58}(\text{n,p})\text{Co}^{58}$ reaction rate along the central axis of the bulk shielding experiment.

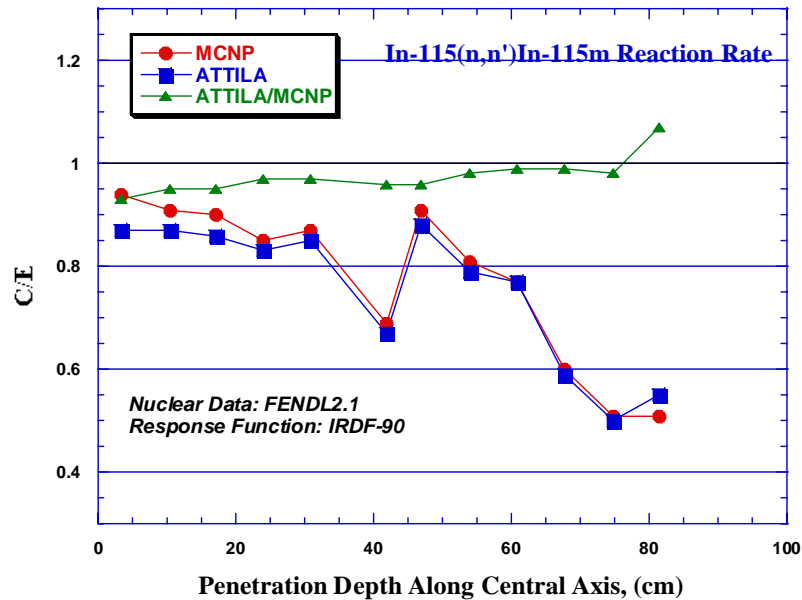


Fig. 20. The C/E values for the $\text{In}^{115}(n,n')\text{In}^{115m}$ reaction rate along the central axis of the bulk shielding experiment.

To quantitatively assess the trends of the calculations, an average estimate of the several C/E values, as obtained by ATTILA and MCNP for a given reaction rate, and for a given experiment, is obtained assuming that the C/E value at each location has the same weight as others. The impact of deviation from experimental data is clearly more severe at locations closer to the incident 14 MeV source, as is the case in fusion blanket, but this equal weight assumption is made here for simplicity.

Table I gives the average estimates for the C/E values for all the reactions considered in the three experiments. In Table II we introduce the least and largest deviation from the experimental data and the difference between MCNP and ATTILA calculations. One observes from Table I that: (1) the deviation from experimental data are generally less in the MCNP case as compared to ATTILA. The least and largest deviation is 1%, and -23% with MCNP and -3% and -25% with ATTILA, (2) ATTILA's predictions are generally less than the experimental data except for the $\text{Au}^{197}(n,\gamma)\text{Au}^{198}$ reaction in the streaming experiment, and (3) when considering the direction of the deviation, the lowest and largest difference between MCNP and ATTILA's results are ~1% and ~12%, respectively, with an average value of ~7%.

The results cited here thus show that the largest deviation of ATTILA's prediction from the measured data at point locations for several reaction rates, whose threshold energies span the fusion spectrum, is ~20-45% (mostly under prediction, see Fig. 20 at the deepest location for the

In¹¹⁵(n,n')In^{115m} reaction). The ATTILA's results are, on the average, less than those obtained by MCNP by ~1-12%.

Table I. Average Estimates for the C/E Values and Deviation from Experiment

Reaction	Calculation Method	Experiment			
		Tungsten	Streaming		Bulk Shield
			Channel	Cavity	
Zr-90(n,2n)Zr-89	MCNP	2%			
	Attila	-6%			
Ni-58(n,2n)Ni-57	MCNP	-1%			
	Attila	-6%			
Nb-93(n,2n)Nb-92	MCNP	1%	-4%	-6%	-10%
	Attila	-9%	-13%	-10%	-13%
Al-27(n,a)Na-24	MCNP	3%	-10%	-7%	-11%
	Attila	-7%	-20%	-11%	-13%
Fe-56(n,p)Mn-56	MCNP	-4%			-11%
	Attila	-14%			-14%
Ni-58(n,p)Co-58	MCNP	6%	4%	3%	-7%
	Attila	-4%	-6%	-3%	-8%
In-115(n,n')In-115m	MCNP	-6%			-23%
	Attila	-18%			-25%
Au-197(n,g)Au-198	MCNP	-1%	3%	7%	
	Attila	-10%	9%	10%	

Table II: The least and largest deviation from experimental values and difference between MCNP and ATTILA calculations

Least Diviation from Experimental Data			
MCNP	~1%	Nb-93(n,2n)Nb-92	Tungsten Experiment
Attila	~-3%	Ni-58(n,p)Co-58	Streaming (cavity) Expt.
Largest Diviation from Experimental Data			
MCNP	~-23%	In-115(n,n')In115m	Bulk Shielding Experiment
Attila	~-25%	In-115(n,n')In115m	Bulk Shielding Experiment
Differences Between Attila and MCNP Results			
Lowest	~1%	Ni-58(n,p)Co-58	Bulk Shielding Experiment
Largest	~12%	In-115(n,n')In-115m	Tungsten Experiment.

II.B Benchmarking with the MCNP CAD Model of ITER

The participants in the nuclear design of ITER have agreed to use a standard CAD model of ITER (shown in Fig. 21) to compare results for five responses selected for benchmarking purposes to test the efficiency and accuracy of the CAD-MCNP approach developed by each ITER party⁴⁻⁶ as well as to benchmark ATTILA for large and complex systems. The “Simplified” ITER benchmark model is a 40° toroidal segment which has 774 volumes and 18116 surfaces. It utilizes a source defined on a 40X40 R-Z grid shown in Fig. 22.

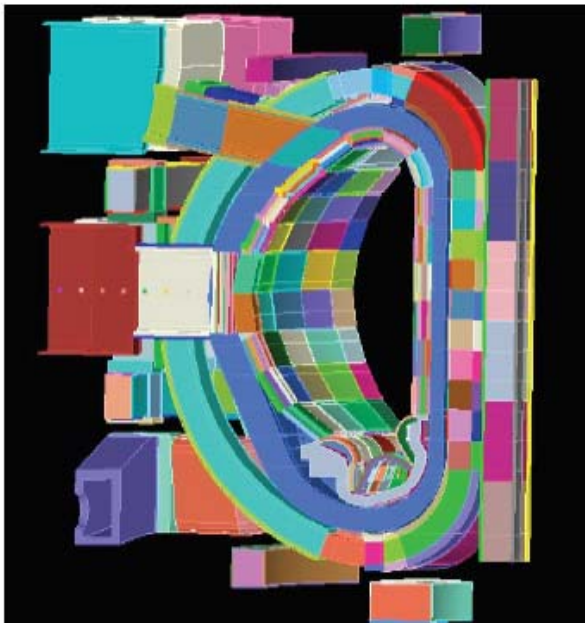


Fig. 21. The simplified ITER benchmark CAD model

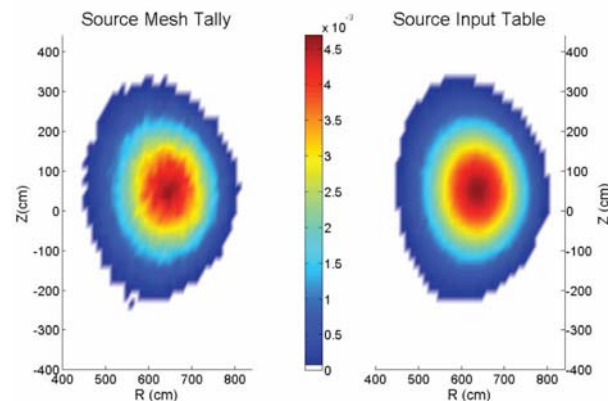


Fig.22. Source characterization

II.B.1 Specifications of the Benchmark:

The specifications of the benchmarks have been issued¹⁸ by the ITER International Team (IT). The five responses calculated with ATTILA for benchmarking with MCNP results are posted at https://mywebspaces.wisc.edu/xythoswfs/webui/_xy-5711042_1-t_NtNCMt80. They are:

- (1) Wall loading at ITER First Wall FW both on the O/B and I/B
- (2) a. Neutron and gamma flux at the divertor surface
b. Heating rate (from neutron and gamma) in the structure material behind the divertor surface
- (3) total heating rate in the inner leg of the TF coil (in each of the 10 equally spaced parts of the straight leg from -399 cm to 404 cm)
- (4) Neutron and gamma flux profile in the dummy shield blanket module (SBM, 5 layers) and in the dummy shield (10 layers) placed in the equatorial port
- (5) Neutron and gamma flux in several locations behind the dummy shield

II.B.2. CAD Model, Meshing, and Cross-Section Library

The CAD model used in the present ATTILA analysis was basically created with Solid Works software based on the model of Fig. 21. The generated 40-degree sector is shown in Figs 23-24. The tetrahedral meshes (cells) generated with ATTILA using layering techniques was ~496,000 meshes. These meshes are shown in Fig. 25.

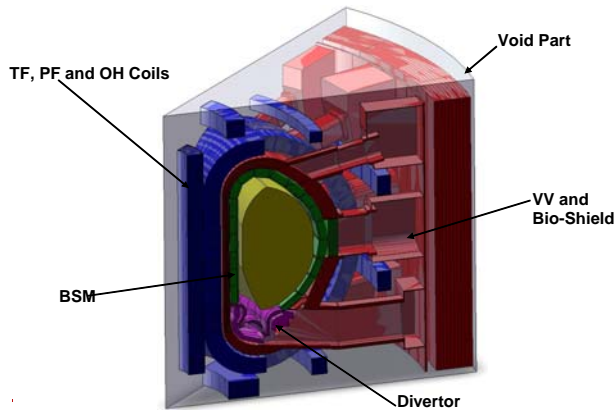


Fig. 23. The 40-degree Solid Works CAD model of ITER used in the present analysis

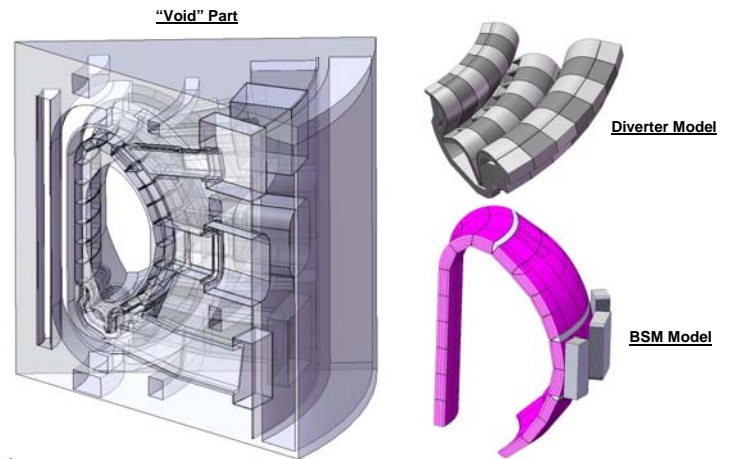


Fig. 24. The BSM and divertor CAD model integrated in the 40-degree CAD model

The conversion of the MCNP plasma source definition (represented by the 40 x 40 grid) into an external volumetric source in a format acceptable by ATTILA was undertaken using a special Python script written by the Transpire Inc., the developer of ATTILA. This script converts the Cartesian coordinates and associated source strength into corresponding values acceptable by ATTILA tetrahedral format. The source strength is depicted in Fig 26. Note that the 500 MW fusion power generated in ITER plasma region corresponds to $\sim 1.97 \times 10^{19}$ neutron/s in the 40-degree sector. This was used as the source normalization factor in the results reported here.

Originally, ATTILA utilized a 175n-47g multi-group library based on FENDL2.1 data-base that was lacking important reaction cross-sections such as the helium and hydrogen production cross-section as well as DPA cross-section. The reaction rates calculated with these cross-sections are the three indicators used to assess the damage in the structural material. In addition, the original library did not explicitly give the heating cross-section (Kerma) for neutron, gamma, and the total. The BBC and TRANSX¹⁹ processing codes were used to correct this deficiency and generate these cross sections from the multi-group FENDL 2.1 basic library posted on the website (<http://www-nds.iaea.org/>) of the Nuclear Data Section of the International Atomic Energy Agency (IAEA.)

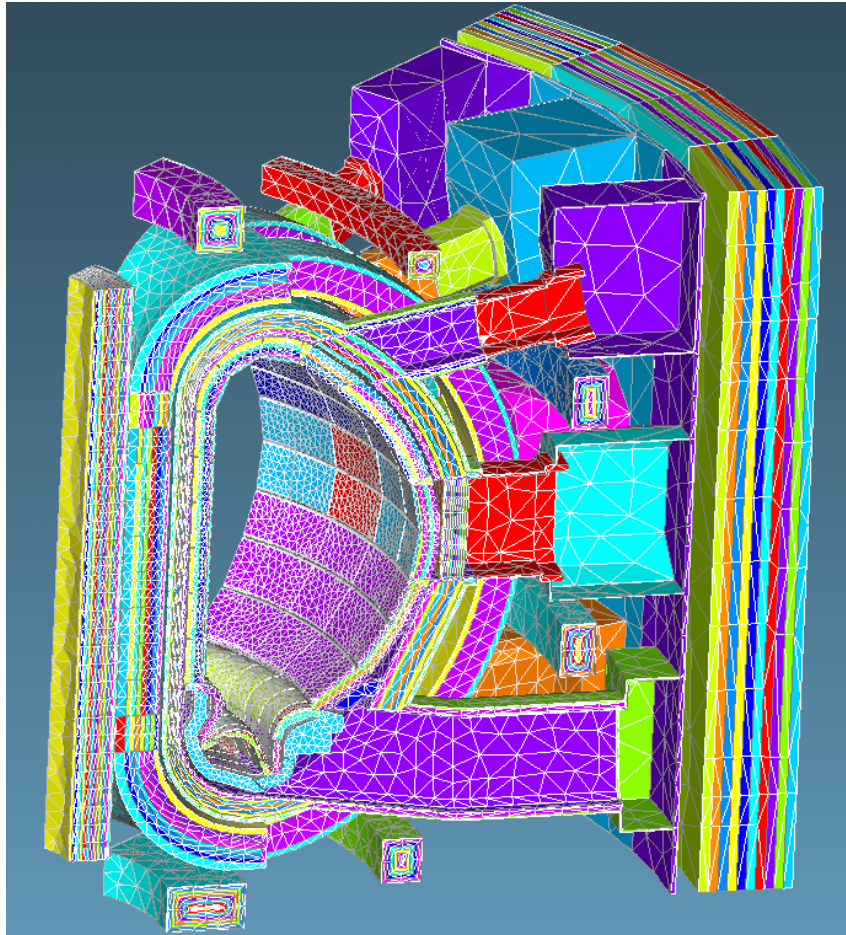


Fig. 25. Mesh scheme in the ATTILA 40-Degree CAD Model

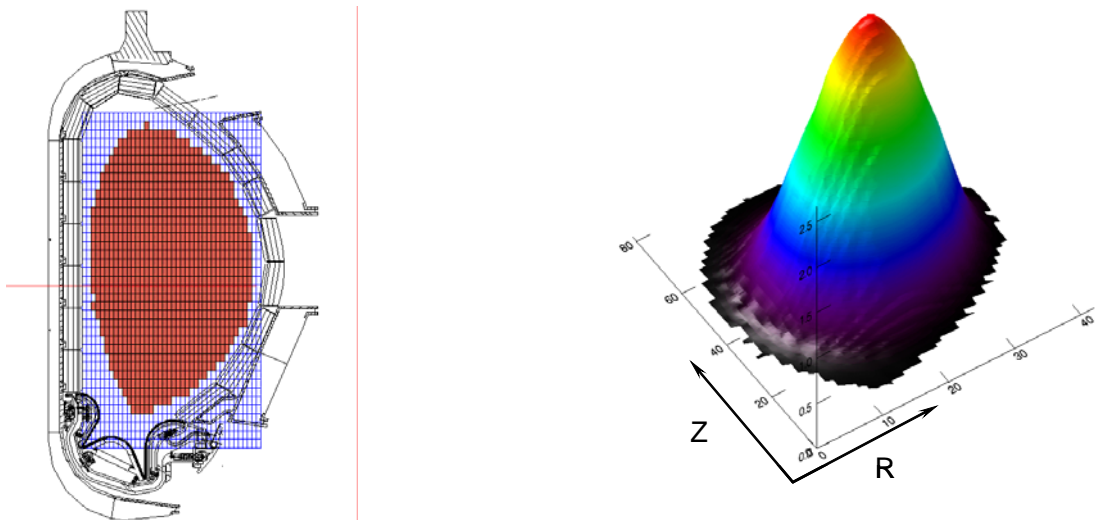


Fig. 26. The 40 x 40 grid plasma source and its conversion to ATTILA Source

II.B.3. Calculation Environment and Procedures

The Opteron LINUX Cluster residing at PPPL (name ITERPPN) was used to perform the transport calculation and providing edit reports and TECPLOT files for visualization of the solution field. It is a dual cores 2.6 GHz 2 processors with total memory of 8 GB. The total Swap between the 8 GB RAM and the hard disk is ~10 GB. One processor was used in the analysis reported here. Future ATTILA runs on the ITERPPN will utilize additional 8 GB RAM (total of 16 GB) and the 4 processors available.

Three runs were completed. The same ~496K cells were used in each run (layered configuration). The P2 scattering order with Galerkin treatment was applied to each run:

(1) Sn4 run:

The 175n-42g FENDL2.1 library was condensed to 72n-24g library (similar to MATXS6 of LANL¹⁹). Because of the relatively large number of neutron-gamma groups used in this run, lower order of angular quadrature was applied (Sn4).

(2) Sn16 runs:

The 175n-42g FENDL2.1 library was condensed to 29n-11g library. Because of the relatively fewer number of energy group, higher angular quadrature was applied (Sn16). It was shown that the solution accuracy is more sensitive to the number of angular directions than to the number of energy groups provided the group boundaries are selected in a way that preserves the resonances and steep changes the cross-section of predominant materials such as iron.

(3) Sn40-Sn16 run:

The 175n-42g FENDL2.1 library was condensed to 29n-11g library (similar to Sn16 run). However, the run was completed in two steps:

- Use 1st neutron group (14.19-13.83 MeV energy boundaries) to generate neutron scattering source everywhere in the model with Sn40 angular quadrature.
- Use the scattering source from above step as an external source for the remaining of the 28 neutron-11 gamma group
- Add flux moments of the two runs to get the total flux moments. Get reaction rates and any nuclear response using the summation of contribution from each run.

The completion of the Sn4 run was achieved after ~10 days (~240 hrs). The Sn16 run was completed after ~7 days (~168 hrs), while ~8.5 days (~204 hrs) was needed to complete the Sn40Sn16 run. The results of the MCNP were well reproduced by ATTILA although few groups (29n-11g) were used with relatively low quadrature set. The main difference is that all the five responses of the benchmarks can be calculated by ATTILA in one run whereas several runs were needed in the case of the MCNP calculations which require different variance reduction technique for each response under consideration¹². For example, the runtime to calculate the wall load, the divertor flux and heating, the TF coil heating and the flux profiles throughout the equatorial port is ~34 hrs, ~50 hrs, 413 hrs, and ~209 hrs, respectively⁵ (total ~706 hrs.) The total of 706 hrs is to be compared to ~204 hrs runtime of the Sn40Sn16 case (a factor of ~3.5 larger). In addition, the TECPLOT files generated by ATTILA enable the visualization of the flux (and any desired response) every where in the model.

II.B.4. Visualization of the Solution Field

The TECPLOT file generated from the Sn40Sn16 run was used to visualize the solution field (neutron flux or its logarithmic value) everywhere in the 40-degree sector. Figures 27-28 show the log of the neutron flux in the model and at various regions/orientation. In the original runs, a normalization factor of 0.1111 was used ($0.1111 \times 1.7753E20 = 1.9723E19$ n/s, the plasma source in the 40-degree sector.) Figures 29-31 show the neutron flux in the plasma and divertor region, in the BSM regions and in the TF Coil leg and the Equatorial Port regions, respectively.

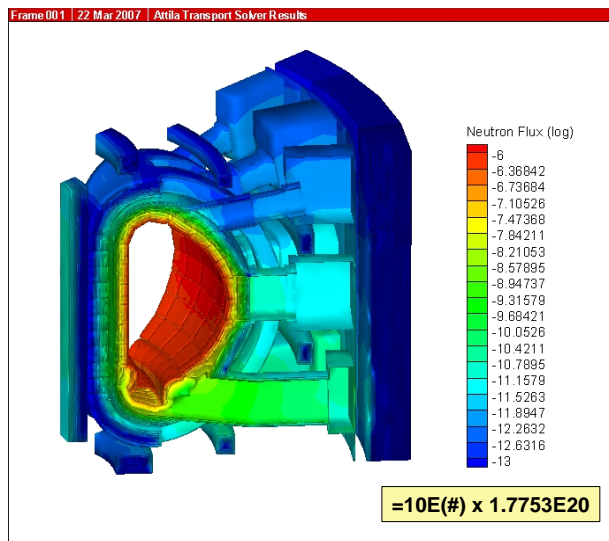


Fig. 27. Neutron flux in the 40-degree sector of ITER sector (1)

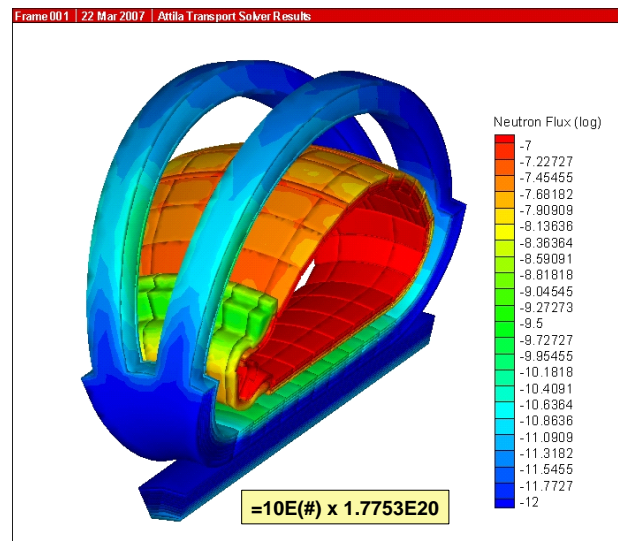


Fig. 28. Neutron flux in the 40-degree sector of ITER (2)

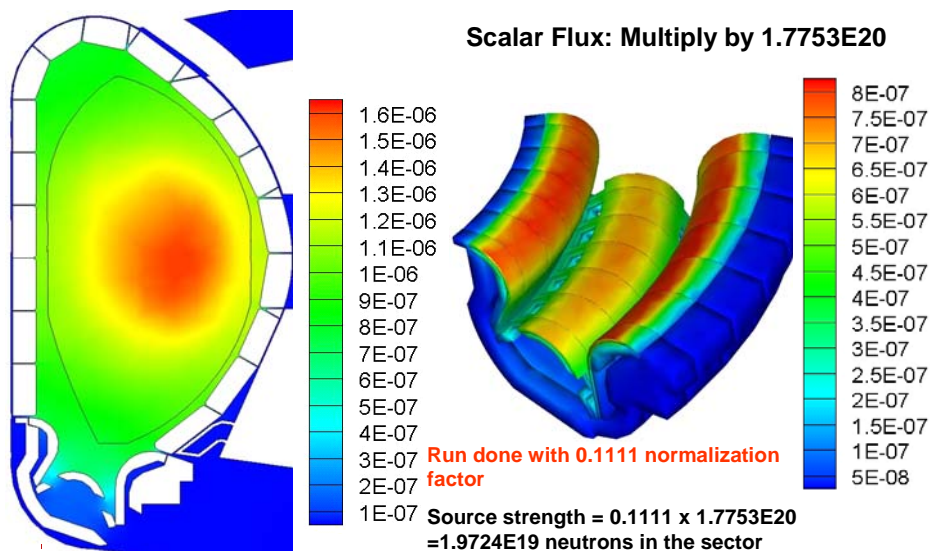


Fig. 29. Visualization of the neutron flux in the plasma and the divertor regions

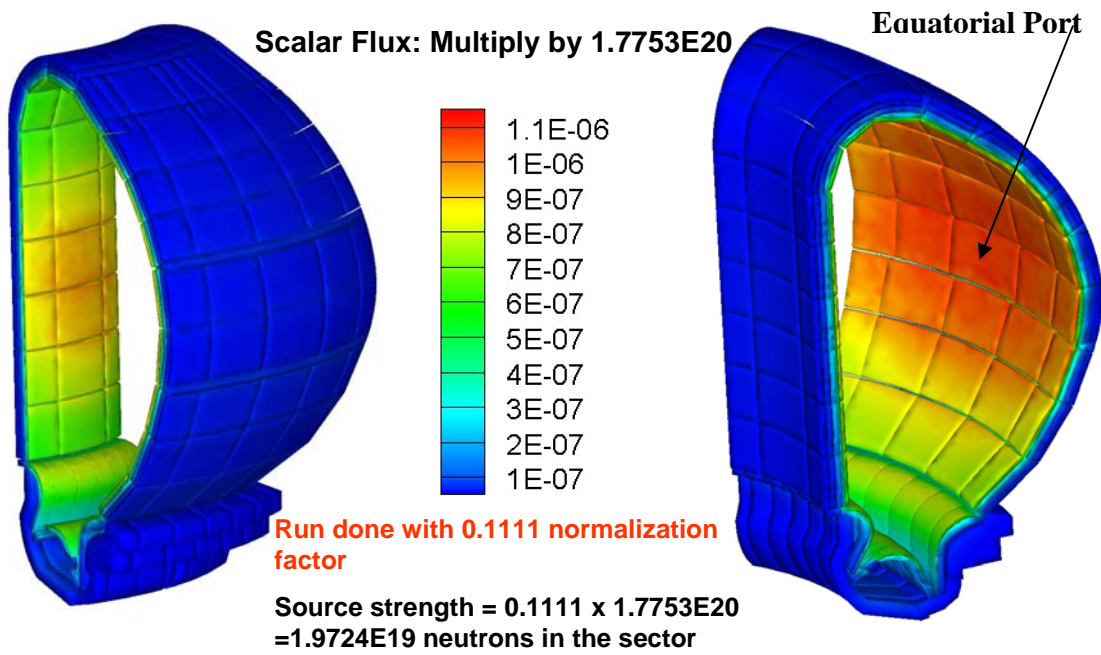


Fig. 30. Visualization of the neutron flux in the blanket shielding modules

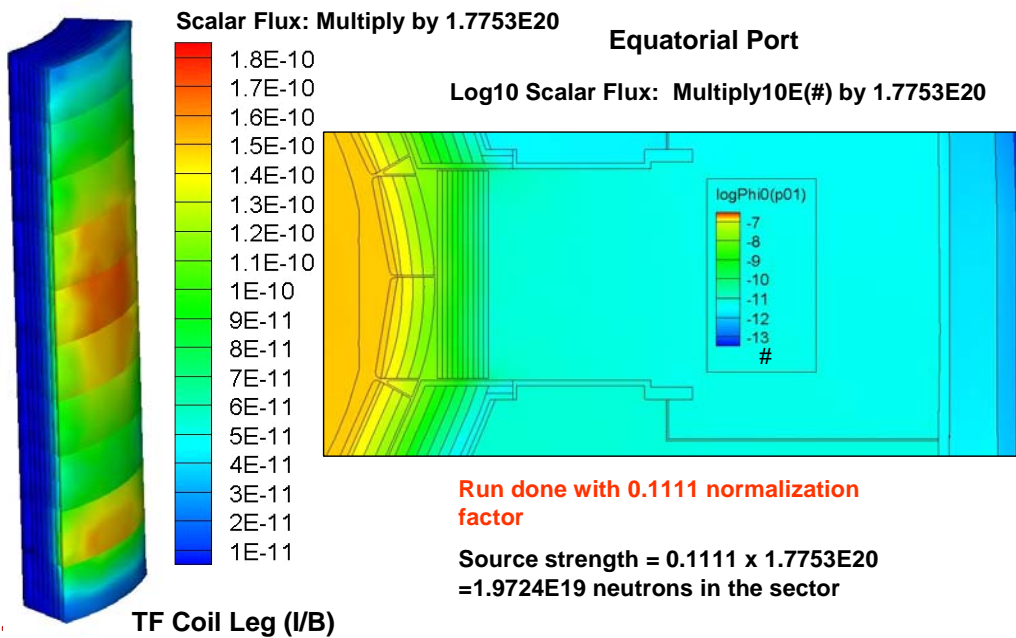


Fig. 31. Visualization of the Neutron Flux in the TF Coil Leg and the Equatorial Port Regions

II.B.5 Benchmarking Results

II.B.5.a Neutron Wall load (NWL)

Figure 32 shows the neutron wall load distribution at each module with comparison to the University of Wisconsin (UW) MCNP calculation. About 34 hrs were needed to calculate the NWL in the UW MCNP case and ~ 8 minutes with ATTILA. The peak values on the Inboard (IB) and Outboard (O/B) with ATTILA are 0.64 MW/m^2 and 0.84 MW/m^2 as opposed to 0.57 MW/m^2 and 0.74 MW/m^2 with UW MCNP (differences of ~13% and ~14% respectively). The values reported in ITER Nuclear Analysis Report (NAR²⁰) are 0.60 MW/m^2 and 0.78 MW/m^2 , respectively. ATTILA's results are thus larger than NAR's results by ~6.6% and ~7.7%. As for the average NWL, the value obtained with ATTILA is $\sim 0.57 \text{ MW/m}^2$ (0.55 MW/m^2 NAR) and $\sim 0.51 \text{ MW/m}^2$ with UW MCNP, a difference of ~11% (~3.6% NAR.)

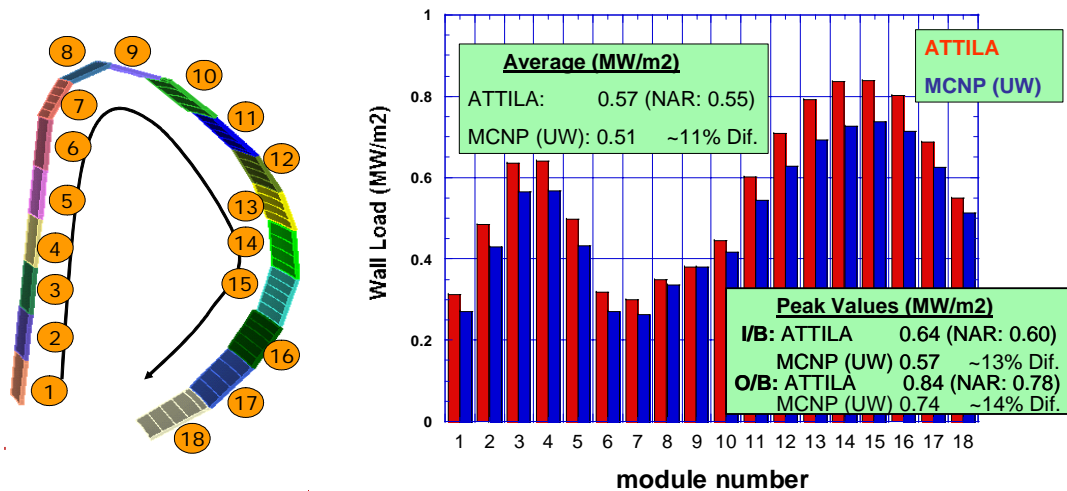


Fig. 32. Neutron wall load (MW/m²) on the surface of each module and comparison to UW MCNP results (40-degree Sector)

II.B.5.b Neutron Flux and Nuclear Heating Rate in the Divertor

The neutron flux ($10^{13} \text{ n/cm}^2 \cdot \text{s}$) and the total heating (kW) in the Inboard Target part, the Central Dome part and in the Outboard part of the divertor are shown in Figures 33, 34, and 35, respectively. The divertor segment shown in these figures is the central segment (one out of seven segments) shown in Fig. 29. The ATTILA's results based on the Sn40Sn16 run are the ones shown in the following figures unless otherwise indicated.

Region 1 in these Figures is made of Cu 20% Vol and W 80% Vol. The regions with inclined surfaces denoted 2 in Figures 33 and 35 are made basically of carbon (99.99% with Fe, Ca, Al, and Ba138 impurities). Region 3 in Fig. 33 (2 in Fig. 34, 3 and 4 in Fig. 35) is made of SS316L(N)-IG 33% Vol, water 7.1% Vol, and Cu 59.9% Vol. The regions behind these layers (denoted 4 in Fig. 33; 3 in Fig. 34; and 5, and 6 in Fig. 35) are made of SS316L(N)-IG 55% Vol and water 45% Vol. The Divertor cassette body is made of SS316L(N)-IG 65% Vol and water 35% Vol.

The neutron flux level in region 2 of Fig. 33 is about half of the level in region 1 (due to its inclination). Due to attenuation, the flux levels in region 3 and 4 are lower as we proceed to the cassette body region. The ATTILA results are larger than those of UW MCNP (statistical errors associated with the MCNP results are shown) by ~3-16% with the largest deviation occurring in the PFC region 1. The total heating rate in the IB target part of the divertor is ~239 kW (ATTILA) and ~207 kW (UW MCNP), a deviation of ~15%.

The prediction of the neutron flux by ATTILA is lower than that of UW MCNP by ~ 0.6-4% in the Central Target part of the divertor (Fig. 34). The total heating rate in the three regions shown in this Fig. is very similar (~268 kW) although lower values (~9.8%) is predicted by ATTILA in the PFC region 1.

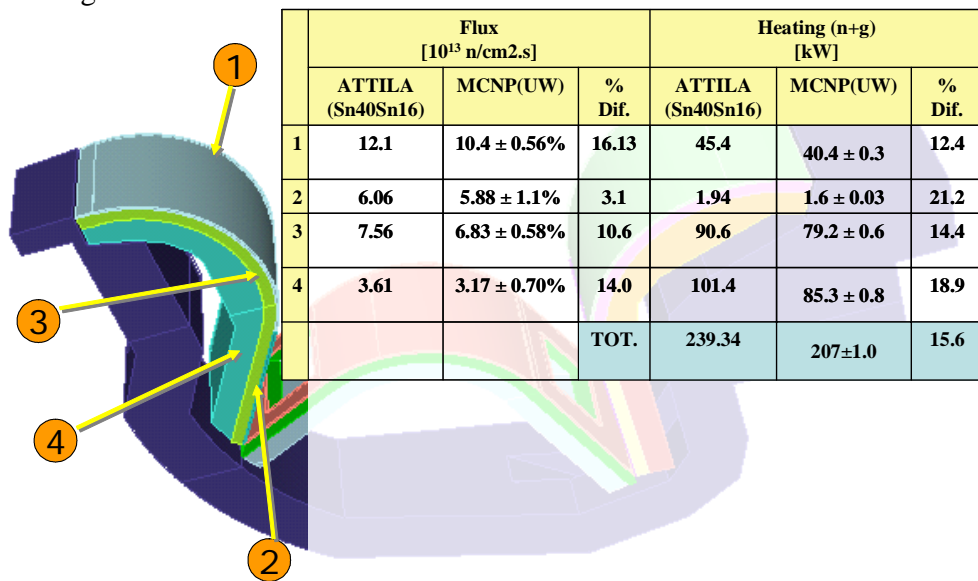


Fig. 33. Neutron flux (n/cm².s) and total heating rate (kW) in the inboard target part of the divertor segment

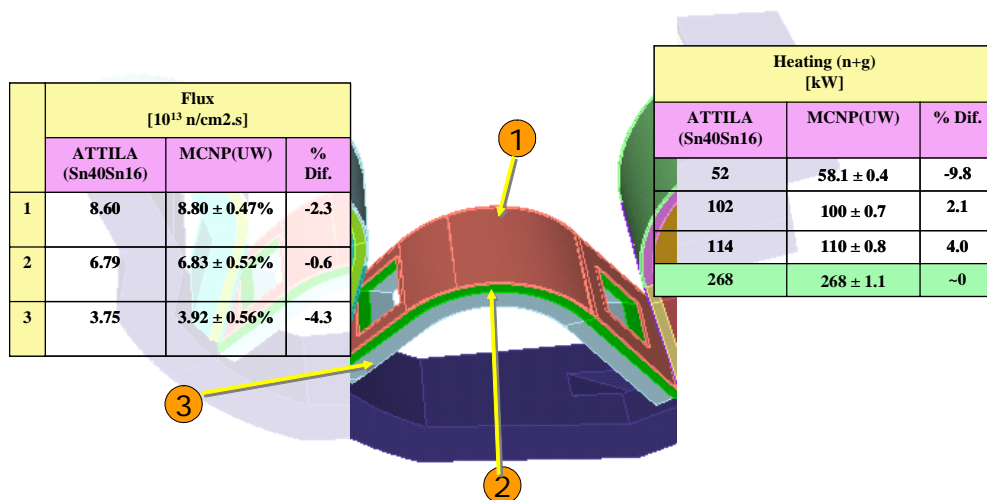


Fig. 34. Neutron Flux (n/cm².s) and Total Heating Rate (kW) in the Central Dome Part of the Divertor Segment

The neutron flux predicted by ATTILA in the OB Target part of the divertor (shown in Fig. 35) is within -10.3% and 1.4% of the values obtained by UW MCNP. The corresponding regional heating rates are within -25% and 8.3%. The total heating rate predicted by ATTILA (~379 kW) is larger than that predicted by UW MCNP by ~ 3.4%.

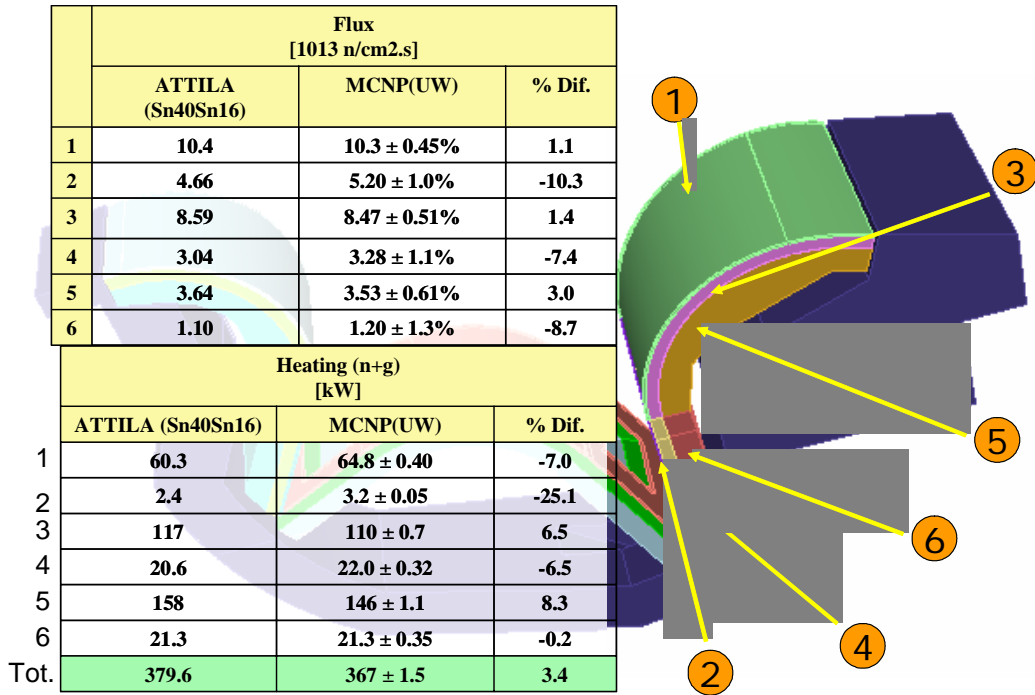


Fig. 35. Neutron flux (n/cm².s) and total heating rate (kW) in the outboard target part of the divertor segment

A summary of the total heating rates in various parts of the divertor segment considered in given in Fig. 36. About 16.8% of the total heat generation rate in this segment (~1067 kW as predicted by ATTILA) is deposited in the cassette body. The total heat generation predicted by UW MCNP is ~1004 kW which is ~3% lower than ATTILA’s prediction. Also shown in Fig. 36 is the average neutron flux in the cassette body. The average value calculated by ATTILA is ~3.18 x 10¹² n/cm².s which is ~ 1% less than UW MCNP prediction.

In ATTILA, various types of edit reports can be produced in the same run. Among these edits are the scalar flux, reaction rates, face flow and current, uncollided wall loading, etc. Also, the type of spatial set chosen for editing is a choice of the analyst. The editing could be by region, by surface, along a line, at points and arcs, etc. One of the responses considered in the present benchmarking exercise is to estimate the “surface” fluxes at the divertor side facing the plasma. ATTILA’s estimations are shown in Fig 37 along with the UW MCNP results.

For surface 1 and 2 of the IB Target part of the divertor, the surface fluxes calculated by ATTILA are $12.82 \times 10^{13} \text{ n/cm}^2\cdot\text{s}$ and $6.77 \times 10^{13} \text{ n/cm}^2\cdot\text{s}$, respectively. These values are larger than MCNP predictions by $\sim 11\%$ and $\sim 5\%$, respectively. The fluxes predicted by ATTILA at surface 6 and 7 of the OB Target part of the divertor are $11.17 \times 10^{13} \text{ n/cm}^2\cdot\text{s}$ and $12.83 \times 10^{13} \text{ n/cm}^2\cdot\text{s}$, respectively (-9% and 11% deviation from MCNP). The divertor surface at the Central Dome part is divided into three sub-surfaces in the ATTILA model. The average surface flux (weighted by the area of each sub-surface) is $9.20 \times 10^{13} \text{ n/cm}^2\cdot\text{s}$ as opposed to $9.47 \times 10^{13} \text{ n/cm}^2\cdot\text{s}$ predicted by MCNP (-2.8% deviation).

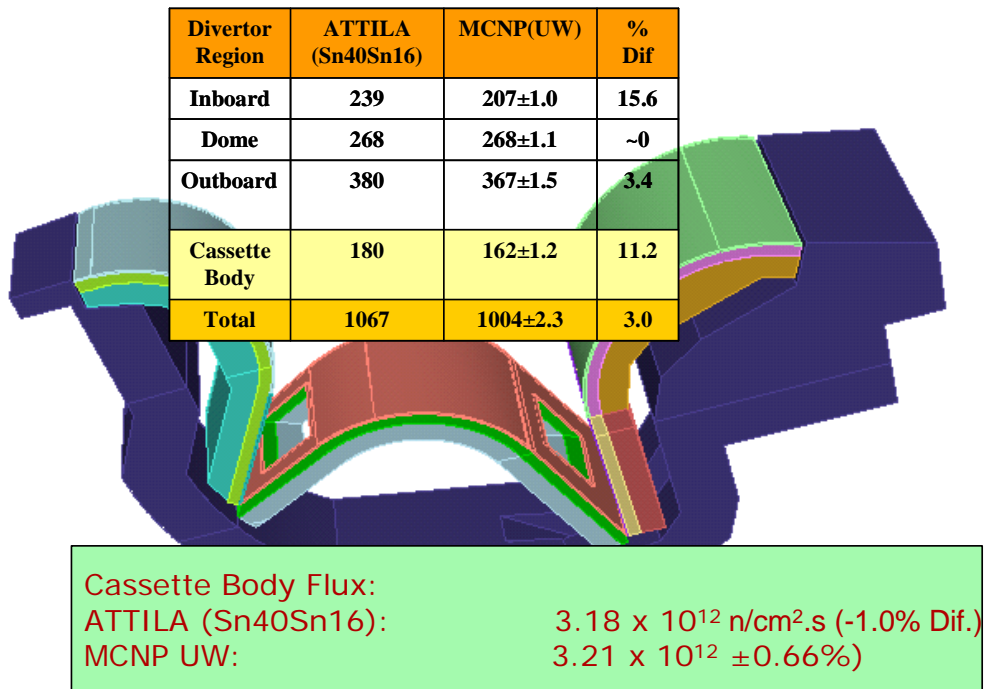


Fig. 36. The Total Heating Rate (kW) in the divertor Segment including the Cassette Body

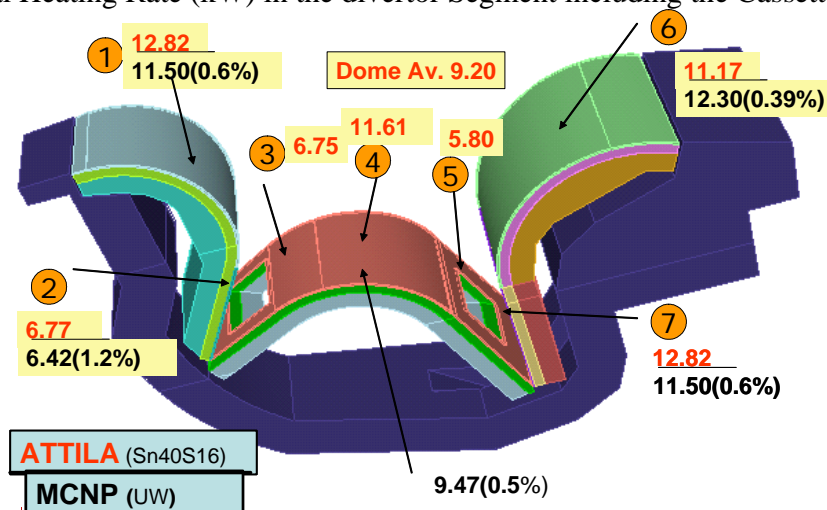


Fig. 37. The divertor neutron surface flux ($10^{13} \text{ n/cm}^2\cdot\text{s}$)

II.B.5.c Flux in the Dummy Blanket Shield Modules and the Dummy Shield Layers Placed at the Equatorial Port

The dummy blanket shield modules (BSM) at the equatorial port consist of 5 layers (~5 cm-thick each) divided into an upper and lower halves. The dummy shield placed behind these 5 layers consists of 10 layers that extend vertically throughout the upper and lower halves of the port. The average neutron flux in the upper halves of the SBM and the dummy shield layers were estimated along with the flux at several (eight) point locations behind the dummy shield. In addition to the total neutron flux, the integrated fluxes in the energy ranges 10 MeV-1MeV, 1MeV-0.1MeV, 0.1MeV-1eV, and below 1eV were also calculated (the ATTILA Sn40Sn16 and Sn16 results are reported).

Figures 38-(a) to 38(e) show the total neutron flux and the integrated fluxes in the energy ranges specified above based on ATTILA and UW MCNP calculations. The ATTILA Sn40Sn16 results are larger (and more accurate) than those obtained from the Sn16 run. The agreement between ATTILA Sn40Sn16 and UW MCNP is good (ATTILA's results are slightly higher) in the dummy BSM and dummy shield layers for the total and integrated fluxes. Behind the dummy shield the total flux with ATTILA Sn40Sn16 is lower by ~11-62% than UW MCNP results. This feature is also exhibited for the integrated flux in the energy range 20MeV-1MeV and 1MeV-0.1MeV (lower by 8-58%, and 9-67%, respectively). Some irregularity in the UW MCNP results can be seen in the integrated flux below 1eV at radial distance 1200 cm.

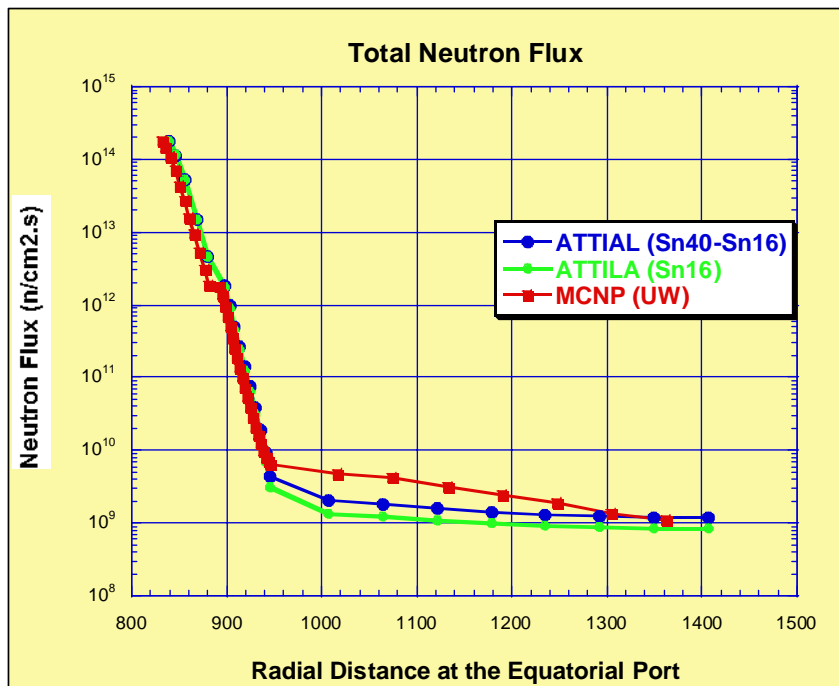


Fig. 38-(a) Total flux in the equatorial port

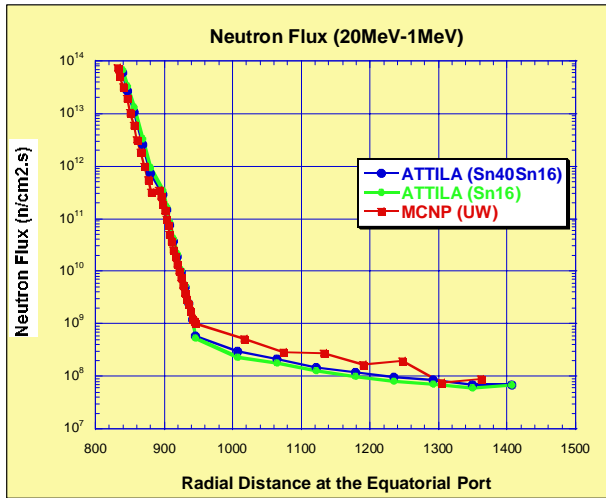


Fig. 38-(b) Integrated flux (20MeV-1MeV)

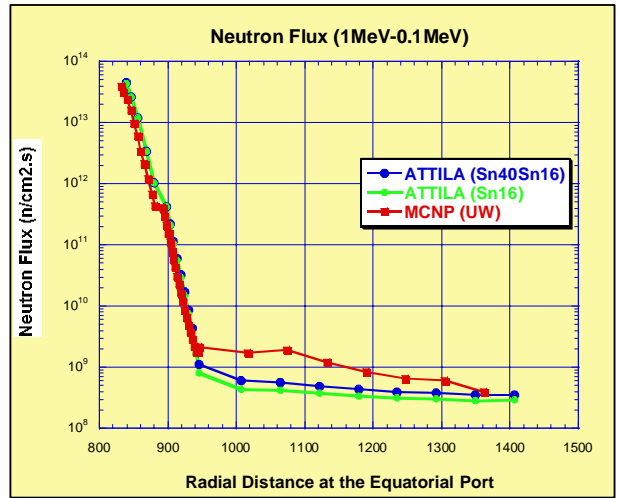


Fig. 38-(c) Integrated flux (1MeV-0.1MeV)

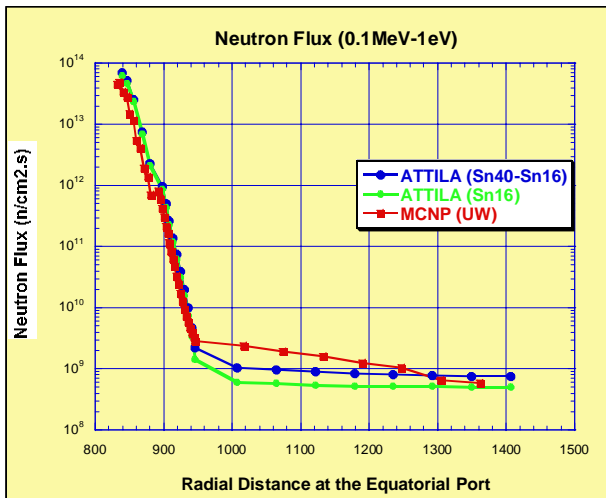


Fig. 38-(d) Integrated flux (20MeV-1MeV)

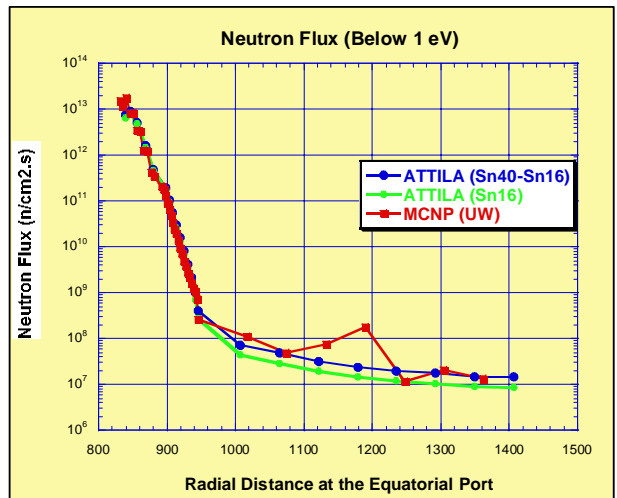


Fig. 38-(e) Integrated flux (1MeV-0.1MeV)

In Table III we summarize the percentage difference between the ATTILA Sn40Sn16 results and the UW MCNP results. The discrepancy is no more than ~20% for the neutron wall load (NWL) and the body/surface flux and total nuclear heating in the divertor. The agreement for the neutron flux in the dummy Blanket Shield Modules and in the dummy shield layers is reasonable. However, larger values (up to 67%) are obtained by the UW MCNP compared to ATTILA's results at the deep locations behind the dummy shield (radial distance greater than ~9.5 m from the torus center).

Table III: Summary of the percentage (%) deviation of ATTILA Sn40Sn16 results from UW MCNP results

Response			% Difference
NWL	Peak		13-14%
	Average		11%
Divertor	Body flux	<i>IB Target</i>	3-16%
		<i>Dome</i>	0.6-4%
		<i>OB Target</i>	1.4% to -10.3%
	Total Regional Heating	<i>IB Target</i>	12-19%
		<i>Dome</i>	-10%
		<i>OB Target</i>	8.3% to -25%
	Total Heating	<i>IB Target</i>	15.60%
		<i>Dome</i>	~0
		<i>OB Target</i>	3.40%
		<i>Cassette</i>	11%
		<i>Total</i>	3%
	Surface Flux	<i>IB Target</i>	5-11%
<i>Dome</i>		-2.80%	
<i>OB Target</i>		11% to -9%	
Equatorial Port	Flux behind dummy Shield	<i>Total</i>	11% to -62%
		<i>20MeV-1MeV</i>	8-58% lower
		<i>1MeV-0.1MeV</i>	8-67% lower
		<i>0.1MeV-1eV</i>	28% to -58%
		<i>Below 1eV</i>	50% to -56%

III. Concluding Remarks

The finite element discrete ordinates code, ATTILA, was recently introduced to the fusion community as a 3D computational tool capable of modeling complex geometries. It is based on generating a CAD model using available design tools (e.g. Solid Work, Pro/Engineer), which is then used as input for subsequent calculations. Spatial discretization is performed through generating user-controlled tetrahedral meshes whose number depends on the degree of accuracy required to account for particle transportation in the media. The code is based on graphic-user-interface (GUI). Design changes (e.g. material assignment, densities, etc.) can be implemented interactively. A post-processing graphic package is used to visualize the nuclear responses in part or in the entire system. Hot spots that do not meet design criteria can be identified and needed changes can be performed in an iterative manner.

This paper gives the results of benchmarking ATTILA's prediction against the experimental data in three fusion-oriented integral experiments performed at the FNG facility, Frascati, Italy, and

against the results obtained by the ITER reference Monte Carlo code, MCNP. In addition, we present ATTILA's results for calculating several responses in large and complex systems such as ITER. This latter benchmarking is necessary to validate ATTILA's capability (and limitations) in solving and storing large flux moments files which normally impose a problem with regard to disk space requirements when the Discrete Ordinates methods are applied for large geometries. This benchmarking and validation exercise was necessary to ensure meeting the quality assurance requirements set forth by ITER Management and Quality Program (MQP).

The results show that the largest deviation of ATTILA's prediction from the measured data at point locations for several reaction rates, whose threshold energies span the fusion spectrum, is ~20-45% (mostly under prediction, with largest deviation occurring at few deep locations.) The ATTILA's results are generally lower than MCNP. The deviation from the MCNP prediction is ~1-12% (~7% average.)

As for benchmarking ATTILA with the MCNP CAD model, the discrepancy with the UW MCNP results is no more than ~20% for the neutron wall load (NWL) and the body/surface flux and total nuclear heating in the divertor. The agreement for the neutron flux in the dummy Blanket Shield Modules and in the dummy shield layers in the equatorial port is reasonable (few % difference.) However, larger values (up to 67%) are obtained by the UW MCNP compared to ATTILA's results at the deep locations. The fact that the UW MCNP results are larger for the flux behind the dummy shield was observed and discussed during the ITER Neutronics Meeting held in Cadarache, France during the period March 26-27, 2007 (https://www.iter.org/bl/WBS_Webs/Safety_Web/Meetings/Neutronics_March07/). By comparison to the other CAD-based MCNP results obtained by ASIPP (China), FZK (Germany), and JAEA (Japan), it appears that ATTILA's results fit well (20-30%) within their values. The UW CAD-based MCNP calculation depends on ray tracing method in which MCNP is called upon from within the CAD model itself where as the ASIPP and FZK MCNP calculation depends on converting the CAD model into input cards readable by MCNP. This over estimation is currently under investigation.

IV. References

1. "DANTSYS 3.0: One-, Two-, and Three-Dimensional, Multigroup, Discrete-Ordinates Transport Code System", *Radiation Safety Information Computational Center, RSICC*, Code Package CCC-547, Oak Ridge National laboratory, Oak Ridge, Tennessee, USA.
2. "DOORS3.2a: One, Two- and Three-Dimensional Discrete Ordinates Neutron/Photon Transport Code System", *Radiation Safety Information Computational Center, RSICC*, Code Package CCC-650, Oak Ridge National laboratory, Oak Ridge, Tennessee, USA.
3. J.F. BREISMEISTER, Editor, MCNP - A General Monte Carlo Code N-Particle Transport Code, LA-13709-M, Los Alamos National Laboratory, Los Alamos, New Mexico (2000).
4. U. FISCHER, A. SERIKOV, H. TSIGE-TAMIRAT, "ITER Benchmark on CAD-MCNP Interface", *Progress Review Meeting on Procedures and Tools for ITER Neutronics*, UW-Madison, WI, USA, July 24-26 (2006).
5. P. WILSON, M. SAWAN, B. KIEDROWSKI, et al., "MCNPX-CGM & the ITER CAD-Neutronics Benchmark", see above reference (2006)

6. "The Progress Review Meeting on Neutronics Analyses for ITER", March 26-27, 2007, Cadarache, France (https://www.iter.org/bl/WBS_Webs/Safety_Web/Meetings/Neutronics_March07/).
7. M. HERMAN AND A. B. PASHCHENKO, "Extension and Improvement of the FENDL Library for Fusion Applications (FENDL-2)", Report INDC (NDS)-373, IAEA, Vienna, (1997).
8. "ATTILA: Comprehensive Radiation Transport Solution Environment" <http://www.radiative.com/ATTILA-010505.pdf>
9. G. FAILLA, "ATTILA Radiative Transport Software", *Review Meeting on Neutronics Analysis Service for ITER*, Frascati, Italy, Dec. 15-16 (2005).
10. M. LOUGHLIN, T. WAREING, A. BARNETT, G. FAILLE, AND G. MCGEE, "Comparison of ATTILA and MCNP for Fusion Applications", *American Nuclear Society Topical Meeting in Mathematics & Computations*, Avignon, France, September 12-15, (2005).
11. M.Z. YOUSSEF, P. BATISTONI, L. PATRIZZI, T. WAREING, AND, I. M. DAVIS "Comparing The Prediction Of "ATTILA" Code To The Experimental Data Of Fusion Integral Experiments and to The Results of MCNP Code", Proceeding of the 17th Conference on the Technology of Fusion Energy,
12. M. Z. YOUSSEF, "Benchmarking ATTILA against Experimental Data", Progress Review Meeting on Procedures and Tools for ITER Neutronics, Madison, Wisconsin, July 24-26, 2006.
13. M. ANGELONE, P. BATISTONI, L. PETRIZZI, M. PILLON, "Neutron streaming Experiment at FNG: results and analysis", *Fus. Eng. & Design*, **51-52**, 653-661 (2000).
14. P. BATISTONI, M. ANGELONE, M. PILLON, L. PETRIZZI, "Compilation of the Tungsten experiment", *The SINBAD 2000 Archive Data Base*, RSICC, ORNL, Oak Ridge, Tennessee, USA.
15. M. MARTONE, M. ANGELONE, M. PILLON, "The 14 MeV Frascati Neutron Generator", *J. Nuc. Materials*, **212-215**, 1661-1664 (1994).
16. "The SINBAD 2000 Archive Data Base" *Radiation Safety Information and Computational Center (RSICC)*, Oak Ridge National Laboratory, Oak Ridge, Tennessee, USA.
17. N. P. KOCHEROV, P. K. MCLAUGHLIN, "The International Reactor Dosimetry File (IRDF-90)", Report IAEA-NDS-141, Rev. 2, Oct. (1993).
18. G. Federici, H. Iida, "Specification for ITER International Benchmark for CAD Based Neutron Transport Calculations, Version 5. January 8, 2006", see Ref 4 and 5
19. R.E. MacFarlane, "TRANSX2: A Code for Interfacing MATXS Cross-Section Libraries to Nuclear Transport Codes", Technical Report LA-12312-MS, Los Alamos National Laboratory, July 1992
20. ITER Nuclear Analysis Report (NAR, 1998, ITER FEAT 2001 and ITER FEAT rev. 2004

Acknowledgment

This work is supported by US ITER System Integration (ORNL), Diagnostics Group (PPPL) and partially by the US Test Blanket Program. The MCNP results of the integral experiments are obtained and provided by the FNG personnel (Batistoni and Petrizzi, et al.) The MCNP results of the ITER CAD model is obtained and provided by the University of Wisconsin personnel (Wilson, et al.) Contribution from Failla and Davis (Transpire Inc.) is appreciated.